A PRACTIONER'S GUIDE TO OPERATIONAL REAL TIME EARTHQUAKE FORECASTING

John B Rundle
Departments of Physics and Geology
University of California, Davis, CA
Open Hazards Group, Davis, CA

James R Holliday, William R Graves, Paul B Rundle,
Daniel E Rundle, Alex Hannon and Charles Graves
Open Hazards Group, Davis, CA

Boris Jeremic and Sashi Kunnath
Department of Civil and Environmental Engineering
University of California, Davis
Open Hazards Group, Davis, CA

Richard Feltstykket
University of California, Davis, CA
Open Hazards Group, Davis, CA

Kevin Mayeda
Berkeley Seismological Laboratory
University of California, Berkeley, CA
Open Hazards Group, Davis, CA

Donald L. Turcotte
Department of Geology
University of California, Davis

Andrea Donnellan
Division of Earth and Space Science
Jet Propulsion Laboratory
Pasadena, CA

ABSTRACT

This paper reviews and discusses a currently operating real time on demand earthquake forecast for California and the world. We describe the forecast method in terms of the standard model of elastic rebound theory of earthquakes, and also provide a guide to its use and interpretation of results. The forecast methodology includes both a forecast and a residential damage estimator and is currently online at www.openhazards.com. A free mobile app ("QuakeWorks") implementing the forecast can be downloaded from the Apple App Store. The earthquake forecast provides a computation of the probability of a major earthquake occurring in a user-defined region over the next 3 months, 1 year, or 3 years. Magnitude ranges of earthquakes calculated for the forecast range from *m*5 and larger, to *m*8 and larger. The forecast probabilities, which can change very rapidly in time, make use of a real-time seismic catalog comprised of the USGS ANSS earthquake catalog, updated with the 30-day real time feed. Calculations are performed daily at about 21:30 Pacific Time and are then updated on the web site at about midnight Pacific Time. Both prospective and retrospective ("backtesting") have been performed on the general forecast methods to determine accuracy and reliability, yielding a 1-year accuracy of about 80%-85% in space and time. Testing has used standard methods of forecast validation and verification developed in other fields. The forecast is used as input to a standard ground motion algorithm, which is then used as input to a published structural damage model. The damage model assumes that structures conform to the International Building Code applicable at the time they were built. The resulting calculations allow the user to obtain an estimate of the probability of an earthquake, the resulting peak ground acceleration, and the likely damage to residential structures having specified properties. In this paper, we focus primarily on the earthquake forecast technology, leaving a discussion of details of the ground motion and structural damage models to future works.

INTRODUCTION

This paper is a practitioner's guide to the understanding and use of the online seismicity-based earthquake forecast system developed by the Open Hazards Group since 2009, and available at www.openhazards.com . A free mobile version of the application ("app") is available from the Apple App Store for iOS7 phones.

FORECASTING AND PREDICTION – WHAT'S THE DIFFERENCE?

To begin the discussion, we provide a more precise definition of these two terms than has usually been available.

- A deterministic prediction can be defined as a deterministic statement that can be verified by a single observation.
- A probabilistic forecast can be defined as a statement of probability that requires multiple observations to establish a confidence level.

An example of a deterministic prediction is the statement, "the next coin toss will turn up Heads". An example of a probabilistic forecast is the statement that "the next coin toss has a 50% chance of turning up Heads". Despite our best efforts, reliable earthquake predictions have not been shown to be possible (Hough, 2010).

EARTHQUAKE DATA AND STATISTICS

The Open Hazards forecast is an on-demand real-time forecast for defined areas rather than specific faults. It uses seismic catalog data and requires a real-time data feed. "Real-time" in this sense is interpreted to mean "on demand". In principle the forecast can be run at any time to yield the most current probabilities. In practice, the forecast is currently computed once daily, and posted to the web site at about midnight Pacific Time. If a true real-time forecast is required, which might be the case for a major earthquake event, the forecast could be run on a cloud computing system having as many compute cores as needed.

Although there exist other catalogs, such as the CMT (CMT, 2014) catalog, these are not usually real-time catalogs. The ANSS catalog (ANSS, 2014), which forms the historical basis for the forecast, is not real-time either, since it requires events to be reviewed for inclusion. However, the digital 30 day feed is real-time (USGS Atom, 2014), so we have combined the real-time feed with the ANSS catalog to produce a real-time catalog that is available for download on the Open Hazards web site under the *Data* tab at the top. Event indentifiers from the real time feed are compared with the identifiers in the current ANSS catalog, and duplicate events are eliminated.

One of the most important aspects of earthquake data is the magnitude-frequency statistics. In Figure 1 below, we show the earthquake cumulative magnitude-frequency relation for the large region of California, Nevada, southern Oregon and northern Baja Mexico, bounded by the latitudes 29^{o} and 42^{o} N, and the longitudes -127^{o} and -113^{o} W, over the time period from 1920 – present (8/7/2014). The data are plotted as log N vs. M, where N is the cumulative number of earthquakes having magnitudes larger than M. The most important feature of this plot is the long linear region from the smallest magnitude M>3 to nearly the largest magnitude, M>7.3. The red solid line is a fit over this interval, resulting in a Gutenberg-Richter *b*-value of $b = 0.925 \pm 0.006$ (the slope is the negative of b). At the large magnitude end, there are 2 earthquakes during this time that had magnitudes of M=7.3, the 28 June , 1992 Landers event, and the 21 July 1952 Kern County event.

Figure 1. Example of a Gutenberg-Richter (GR) cumulative magnitude-frequency for a large region and over a long time interval encompassing earthquakes up to magnitude M7.3. Recall that a cumulative magnitude-frequency relation represents the number of earthquakes having a magnitude greater than or equal to the magnitude indicated on the abscissa. Here the GR relation is for the large region of California, Nevada, southern Oregon and northern Baja Mexico, bounded by the latitudes 29^{o} and 42^{o} N, and the longitudes -127^{o} and -113^{o} W, over the time period from 1920 to August 7, 2014. The data are plotted as log N vs. M, where N is the number of earthquakes having magnitudes larger than M. The GR b-value for this Figure is: $b = 0.925 \pm 0.006$. At the large magnitude end, there are 2 earthquakes during this time that had magnitudes of M=7.3, the 28 June , 1992 Landers event, and the 21 July 1952 Kern County event.

From Figure 1, it can be seen that the M7.3 earthquakes fall below the red solid line ("scaling line"), implying a relative deficiency of such large events. In fact, we can extrapolate the red solid line to the horizontal axis (single event level) as shown by the red dotted line. We see that the intersection is just less than about M~8, approximately the magnitude of the 18 April 1906 M7.8 San Francisco earthquake, and the 9 January 1857 M7.9 Fort Tejon earthquake. This scaling line would be more "complete" with the occurrence of such a large earthquake and its aftershocks. Completing, or "filling in", the Gutenberg-Richter relation is the essential heart of the Natural Time Weibull forecast method that we describe below (Rundle et al., 2012; Holliday et al., 2014). Typically, this kind of compilation of frequency-magnitude statistics, and extrapolation to the largest possible event, can be justified for time intervals approximately equal to the recurrence time interval for the largest earthquakes that occur in the region (time interval for the "earthquake cycle").

Figure 2. Example of a GR cumulative relation over a small region and a short time interval between two large earthquakes. This GR plot is for earthquakes within 200 km of the location centered on latitude 40.67^{o} N , longitude -125.01^{o} W, off the California coast. There were two recent earthquakes, an M6.5 on 10 January 2010, and a second M6.8 earthquake on 10 March 2014 within that 200 km radius circle. Figure 2 is very different from Figure 1, in that there is again a short scaling or linear region at the small magnitude end, but the intermediate and large magnitude events all fall well below the extrapolation of the scaling line. There is a very clear deficit of intermediate and larger magnitude earthquakes having magnitudes M>4.5 relative to the linear extrapolation implied by the small magnitude events. The GR b-value for line in this plot is:
$b = 0.531 \pm 0.013$

Whereas Figure 1 is representative of Gutenberg-Richter statistics over large regions and long times, Figure 2 is an example of GR statistics over much smaller areas and shorter times. Several M>6 earthquakes have occurred off the coast of northern California in the area of the Juan de Fuca plate boundary and plate tectonic spreading center. We consider two of these events in particular, with the first being the 10 January 2010 M6.5 earthquake with epicenter at 40.65^{o} N latitude, -124.69^{o} W longitude. The second event is the 10 March 2014 M6.8 earthquake with epicenter at 40.83^{o} N latitude, and -125.13^{o} W longitude.

Figure 2 shows the GR relation including only the events after the M6.5 first earthquake and before the M6.8 second earthquake. Figure 2 is very different from Figure 1, in that there is again a short scaling or linear region at the small magnitude end, but the intermediate and large magnitude events all fall well below the extrapolation of the scaling line. There is a very clear deficit of intermediate and larger magnitude earthquakes having magnitudes M>4.5 relative to the linear extrapolation implied by the small magnitude events.

The solid red line in Figure 2 shows the magnitude range of the linear fit, from M3 to M4, and the red dotted line is the extrapolation to larger magnitudes. Note that the b-value of the scaling line in Figure 2, $b = 0.531 \pm 0.013$, is also very different from that in Figure 1. In general, b values over smaller regions can often be variable over similar ranges. Using the idea that the deficit in large earthquakes must eventually be removed over a longer period of time, one would expect that larger magnitude events must occur. This idea is the basis of the Natural Time Weibull method of earthquake forecasting as we describe in the following as we describe in the following section.

EARTHQUAKE CYCLE AND CHARACTERISTIC EARTHQUAKES

One of the most fundamental ideas in earthquake mechanics is the cycle of stress accumulation and release on major faults (e.g., Scholz, 1990). A simple version of the basic idea is shown in Figure 3, which represents the (hypothetical) evolution over time of a single isolated fault subject to stress accumulation due to plate tectonic forces (see, for example, the similar fig. 5.13 of Scholz, 1990). The basic parameters are a failure stress threshold σ_F and a recurrence or cycle time interval T.

Figure 3. A classic representation of the time history of stress and slip on a simple isolated earthquake fault. Although the exactly repetitive nature of the stress and slip are now known to be an inaccurate, the basic ideas illustrated here are generally thought to represent the basic features of the earthquake cycle. The top plot shows the time history of stress accumulation and release, and the bottom plot shows the time history of cumulative slip on the fault. In the model, sudden slip occurs when the fault stress $\sigma = \sigma_F$, where σ_F represents the strength of the fault. During the earthquake, the slip suddenly increases (bottom figure), and the stress decreases to the residual value $\sigma = \sigma_o$. Two times are shown in the Figure 3, t_1, a time just prior to the earthquake, and t_2, a time just after the earthquake. T is the recurrence interval between earthquakes.

As the plates move due to convective motions in the earth's mantle, the stress on the fault rises from $\sigma = \sigma_o$ towards the failure threshold σ_F , where $\sigma_F > \sigma_o$. When the failure level is reached, $\sigma = \sigma_F$, the fault ruptures and stick slip frictional sliding occurs. The stress is reduced back to the residual level $\sigma = \sigma_o$ and the earthquake cycle commences again. Figure 3 shows both the variation of stress with time in this simple model (top), and the stair-step increase of fault slip with time (bottom). This simple model of earthquake occurrence is known not to be an accurate model of real earthquakes, as is suggested by fig. 5.13 of Scholz (1990) and discussion therein. This is due to the occurrence of stress interactions between faults, originally discussed in Rundle (1988a, 1988b). However, the essential feature of elastic rebound, leading to a lower stress following an earthquake, is widely accepted.

Suppose we wish to compute the probability of an earthquake over a future time interval Δt that is short compared to the recurrence interval T, $\Delta t \ll T$. An example would be T=200 years and Δt= 1 year. Referring to Figure 3, we would like to compare the 1-year pre-event probability $P(t_1 \mid \Delta t)$ of an earthquake computed at time t_1 just before the last earthquake, with the 1-year post-event probability $P(t_2 \mid \Delta t)$ just after the next earthquake. Based on the model of Figure 3, one would expect that :

$$P(t_2 \mid \Delta t) < P(t_1 \mid \Delta t) \tag{1}$$

(i.e., probability of the same just-occurred event decreases after the earthquake). Equation (1) is a defining characteristic of the Open Hazards forecast model.

TYPES OF FORECAST

In California, previous forecasts have been carried out by the Working Group on California Earthquake Probabilities (WGCEP, 2014; Field, et al. 2014). These are fault-based forecasts, meaning that the major earthquakes in the future are assumed to occur on known faults that are included in the model. Probabilities are computed for each defined fault in the model.

This type of forecast then requires considerable data on past earthquakes on each fault in the model, data that is often not available and may never be available. Examples of the type of data required are earthquake recurrence intervals, slip statistics, and dates and spatial extent of all past ruptures. An additional reason that previous forecasts are based on fault-slip statistics is related to the desire to conform to the inputs required by the risk modeling damage and loss models, such as HAZUS (2014). In California, these models use the WGCEP forecast models to run scenario computations for ground shaking inputs to the damage and loss calculations.

By contrast, the Open Hazards earthquake forecast is a seismicity-based forecast that computes probabilities in defined spatial areas using the Natural Time Weibull method (NTW: Rundle et al., 2012; Holliday et al., 2014). The NTW method is a routinely automated operation, updated in real time, and is globally available via a readily accessible User Interface (UI).

The Natural Time Weibull (NTW) method (Rundle et al., 2012; Holliday et al.,2014) is based on the idea that the Gutenberg-Richter magnitude-frequency distribution is a universal property of earthquake seismicity. Over any reasonably long time interval, and in any spatial region, the GR relation is characterized by statistics as shown in Figure 1. Over shorter time intervals and in more local regions however, the statistics can show a deficit of large earthquakes as in Figure 2. Over time, this deficit must be rectified. Alternatively we can say that the method relies upon "filling in" the large earthquake deficit.

To explain in more detail, consider the Gutenberg-Richter magnitude-frequency relation:

$$N = 10^{a} 10^{-bm} \tag{2}$$

Here N is the number of earthquakes whose magnitudes are greater than or equal to m, and a and b are parameters for the region under consideration. Parameter a expresses the overall number of earthquakes larger than the minimum catalog completeness level. Parameter b determines the number N_{SL} of small earthquakes with magnitude m_S corresponding to each large earthquake of magnitude m_L:

$$N_{SL} = \frac{10^{a}10^{-bm_S}}{10^{a}10^{-bm_L}} = 10^{b(m_L - m_S)} \quad (3)$$

The basic idea of the NTW method can be discussed most easily when the GR b-value is $b = 1$. In that case, there are $N_{SL} = 1000$ small earthquakes having $m_S = 3$ or greater for every large earthquake with $m_L = 6$ or greater. Thus after a large earthquake $m_L \geq 6$ occurs in a region, we begin counting small earthquakes having magnitudes $m_S \geq 3$. When eventually another 1000 such earthquakes have occurred, the Gutenberg-Richter relation implies that it is about time for another large earthquake $m_L \geq 6$. We then use Weibull statistics to convert this count of small earthquakes into a probability.

The small earthquake count is rather like a clock counting down the seconds leading up to "striking the hour", with the occurrence of the large earthquake. The small earthquakes represent natures' *natural time* clock that marks the occurrence of the large earthquakes. Viewed from this perspective, the primary problem is to map the natural time count to the passage of calendar time.

The method also accounts for the spatial correlations between earthquakes in a region. The occurrence of both aftershocks and triggered seismic activity indicates that earthquakes influence the occurrence of one another through the medium of stress transfer. Thus earthquake occurrence is correlated over finite spatial distances. The NTW model assumes that the correlation length ξ is fixed at a distance corresponding to the average source dimension of the largest earthquake in a region (Rundle et al., 2012; Holliday et. al., 2014). Since generally the largest earthquakes have source dimensions of 200-600 km (with some rare exceptions), we set the correlation length $\xi = 400\ km$. Future improvements of the forecast model may involve determining a different value of ξ for each region. For California, $\xi = 400\ km$, since both the 1906 and 1857 earthquakes were of approximately this length (Scholz, 1990).

TESTING AND ACCURACY

One of the motivations for producing the seismicity-based forecasts such as NTW is that they can be automated and systematically tested. The fault-based forecast models could not be systematically tested, since they were based in large part on expert opinion. Forecast validation and verification are terms originated by the World Climate Research Program that have developed or adapted most of the important testing methods (WCRP, 2014; Joliffe and Stephenson, 2003). The most commonly used tests are the Reliability/Attributes and Receiver Operating Characteristic tests based on the Briar score of forecast skill.

These and the other popular tests in general make no assumption about the statistics of the data or the models that are used to forecast future evolution of events. This is different from Likelihood tests that must assume that the statistical structure of the data is known, a disadvantage (e.g. Bevington and Robinson, 2003). Likelihood tests must also assume that the data (earthquakes) are independent and uncorrelated. This assumption is known to be false, since earthquake triggering, aftershocks, and other phenomena indicate that earthquakes interact via stress transfer, sometimes over considerable distances.

The most recent example of prospective earthquake testing is the Relative Earthquake Likelihood Model (RELM) test (Field, 2007). This test involved 17 forecast models that were submitted to a central repository in 2005. The models were evaluated on their ability to forecast the location and other characteristics of the future M>4.95 earthquakes within the region of California and northern Baja California (Mexico) during the 5 year period from January 1, 2006 to December 31, 2010.

At the close of the testing period, all of the forecasts were made available for evaluation via a variety of tests. 5 of the 17 forecasts were classified as forecasts of mainshocks + aftershocks, while the remaining 12 were classified as mainshock-only forecasts. One of the 5 mainshock-aftershock forecasts was developed by Holliday et al. (2007) and is part of the method upon which the NTW forecast is based.

This Holliday et al. (2007) forecast came the closest to forecasting the actual number of future events. That forecast anticipated 30 events, whereas 31 actually occurred. Two of the evaluation methods that were applied to the forecasts used testing methods that did not assume *a priori* anything about the statistics of the data or forecast (Lee et al., 2011; Zechar and Zhuang, 2014). Both of these found that the Holliday et al. (2007) forecast performed the best.

The RELM test was established to provide a test of forecasts of spatial locations of future significant earthquakes. Holliday et al. (2005) and Rundle et al. (2007) showed that between 85% and 93% of future earthquake locations could be successfully forecast to occur in only a small fraction of the geographic area. The larger the forecast area allowed, the higher the fraction of successful forecasts.

In the Holliday et al. (2005, 2007) methodology, the fraction of forecast area ranges between 2.5% and 15% (e.g., Rundle et al 2007; Holliday et al., 2005). A forecast is obviously more likely to be successful if the forecast area is larger. The fact that the forecast area represents only a small fraction of the geographic area is a direct result of the observational fact that earthquake activity tends to be highly concentrated, or clustered in space.

Forecasting earthquake activity in time is more difficult than forecasting earthquake activity in space. Temporal reliability and skill can also be verified by Reliability and Receiver Operating Characteristic methods as described above. The temporal ROC tests show in particular that the NTW forecast typically performs better than 85%-90% of any competing random forecast, about the same average accuracy as 4-day weather forecasts (Joliffe and Stephenson, 2003; WCRP, 2014). (It should also be noted that it is not known in advance which of the random forecasts are best). Details can be found in Rundle et al. (2012) and Holliday et al. (2014).

WEB-BASED INTERACTIVE FORECASTING

Real-time earthquake forecasts have been generally unavailable to the public or even the practicing engineer, unlike, for example, weather forecasts. In recent years, the standard of practice has been for information to be made available through simple and intuitive web site and mobile applications ("apps"). This is the practice that has been adopted for the Open Hazards web site at www.openhazards.com and iOS app ("QuakeWorks").

GUIDE TO THE WEB APPS – PERSONAL EARTHQUAKE FORECAST (www.openhazards.com/forecast)

We first consider the simplest app, the **Personal Earthquake Forecast**, which can be accessed by placing the mouse cursor on the *Web Apps* menu at the top to see the drop-down menu (Figure 4). Here the user simply enters a location, a set of latitude-longitude coordinates, or other information to designate a location. The app is set initially to geo-locate the user.

Figure 4. Personal Earthquake Forecast tool centered on the location of San Francisco, California. Small red star is the epicenter of the 24 August 2014 M6.0 south Napa earthquake. Low resolution global forecast contours are shown.

The app displays both the global forecast contours that are updated every night, together with a table of probability calculations for 1 month, 1 year and 3 years into the future from the current date. Probability calculations are displayed for events having magnitudes $m \geq 5$, $m \geq 6$, $m \geq 7$ and $m \geq 8$. The date and time of calculation are given at the bottom.

GUIDE TO THE WEB APPS - HAZARD VIEWER (www.openhazards.com/viewer)

Basic Earthquake Forecast. We next consider the earthquake hazards viewer at www.openhazards.com/viewer. Using this page (Figure 5 through 8), the user can calculate earthquake probabilities for California or any other location in the world. Here are the steps. We will first use the *Circle Selection Tool* to define a circular region. Please refer to Figures 5 through 8 as well.

1. Roll over the the *Tools* tab at the top to see the drop down menu. Click on the tab "Earthquake Viewer".

2. The user will see a Google map. Look to the left side of the map. Under the "Earthquake Hazard" heading, locate the *Circle Selection Tool*. Click on the adjacent radio button to the left side.

3. Now click on the map. A dialog box will appear with the heading *Selection Radius*. This tells the user how big the circle will be. The default is 100 km radius. If that is acceptable, click on *Enter*. If that is not acceptable, the user can either enter another radius in km, or wait until the next step below.

4. A large blue circle will appear over the map. There are two yellow crosses, one at the center and one at the right hand edge (Figure 5)

- The user can move the blue circle around by putting the mouse arrow on the center yellow cross, holding down the left mouse, and moving the circle.
- The user can also change the size of the circle by putting the mouse arrow on the right yellow cross, holding down the left mouse, and moving the mouse to expand or contract the circle.

Figure 5. Hazard Viewer tool illustrating the use of a selection circle of radius 100 km around San Francisco, California, with additional display of forecast contours and UCERF2 fault system. The selection circle encompasses the epicenter of the 24 August m6.0 south Napa earthquake at upper right center of the circle (small red star). the calculations indicate that there is a 2.3% chance of a $m \geq 6$ earthquake within the selection circle within 1 year from September 3, 2014 (i.e., the period from September 3, 2014 to September 2, 2015). There is a 1.3% chance of an $m \geq 7$ earthquake during the same time period. Probabilities rise for the longer time interval of 3 years.

5. If the circle is left in place for a few seconds, earthquake probabilities for events occurring in the blue circle will be automatically computed and displayed in a table at the bottom left side of the map. The user will see earthquake probabilities for magnitudes $m \geq 5$, $m \geq 6$, $m \geq 7$ and $m \geq 8$, and for future time intervals of 1 month, 1 year, and 3 years (Figure 5).

6. To make the blue circle disappear, the user should click anywhere on the circle and then answer *OK* in the dialog box.

7. If the user wishes to display earthquake probabilities as spatial contours, sh/e can click on the *Select Forecast* button/bar above the *Earthquake Hazard* box. There are two forecasts, a high resolution (0.1^o x 0.1^o) California forecast, and a lower resolution (0.5^o x 0.5^o) World forecast. These are selected by clicking on them. The user can also "roll time back" by picking an earlier year and month to see how the spatial contours appeared at earlier times. Click on the date boxes to activate dropdown menus for this function.

8. The *Polygon Selection Tool* can also be used in place of the *Circle Selection Tool* to define an irregular polygonal region. Click on the radio button for *Polygon Selection Tool.* Then begin clicking on the map to produce the edges of the polygon. Double clicking on the map will close the polygon. Again, the table of forecast probabilities will be computed and displayed in the lower left corner.

9. California counties can be displayed by clicking on the dropdown menu in the *Locations* section, and then highlighting the desired county.

Benioff Strain Timeseries. Once a circle or polygon has been used to define a small region, the Benioff strain (e.g., Bufe and Varnes, 1993) and forecast timeseries can be displayed by clicking on the *View Strain* bar/button (Figure 6). The chart is displayed in a pop-up using an app adapted from those used to display financial timeseries.

Figure 6. Benioff strain release time series for events in the selection circle of Figure 5. The small yellow icon at lower right corner represents the 24 August 2014 M6 Napa, California earthquake. Magnitudes of earthquakes larger than 2 are also shown as a function of time from 2005 to present. The large step in strain release at the upper right hand side is due to the Napa earthquake.

Pop-ups must be disabled on the browser in order to see the resulting chart. Note that different browsers treat Javascript and other scripts in differing ways, and there are other features such as timeout intervals that are different. We have found that the optimal browser to use in general is Firefox, which is most compliant with the open standards.

The Benioff strain is a measure of the strain release and is derived from taking the square root of seismic moment of a series of earthquakes and summing over time. The strain is revealed as a stair-step series of increments. Large earthquakes will release large strain (and stress), and will appear as large steps. Small earthquakes release small Benioff strain and appear as small steps. Interesting patterns in some areas can be seen, in which strain release appears to increase prior to large earthquakes (activation) or decrease prior to large earthquakes (quiescence).

Note that magnitude vs. time is also displayed in the middle of the chart for the earthquakes that have occurred during the time period. Events larger than magnitude 6 are flagged by a yellow icon. At the bottom a simple version of the time series is also displayed just above the controls that allow limited portions of the time series to be displayed.

Earthquake Probability Timeseries. Another important timeseries can be displayed using the *Forecast Timeseries* bar/button, once the circle or polygon has been used to define the small region (Figure 7). Clicking on the bar/button initiates an action that accesses the database to display the time-varying chance of an earthquake occurring within the selection circle, within the next year from the date given along the bottom time axis.

Once the bar/button is clicked, a pop-up window will appear with the chart app. Radio buttons for $m \geq 5$, $m \geq 6$, or $m \geq 7$ earthquakes are given along the bottom of the pop-up. Note that as the size of the selection region increases, the time to generate the chart increases as well, and may exceed the browser setting for timeout. In that case, the refresh link at the top of the chart pop-up can be clicked as many times as needed. Alternatively, the size of the selection region may be decreased, and the process repeated until a chart appears. Figure 7a,b show probability timeseries for $m \geq 6$ and $m \geq 7$ earthquakes in the selection circle.

Figure 7a. Monthly timeseries illustrating the variation in time of forecast probabilities for $m \geq 6$ earthquakes within the selection circle for time interval of 1 year. The small yellow icon at lower right corner represents the 24 August 2014 m6.0 Napa, California earthquake. The M6 Napa earthquake caused the $m \geq 6$ probability to decrease, similar to Figure 3. A general trend of declining probability can also be seen, which is due to the occurrence of other large events in the region, outside the selection circle. These other large events influence the probability inside the selection circle by means of the correlation length ξ as described in Holliday et al. (2014). If events in the region become less frequent, the overall probability in the circle will tend to decrease over time, and conversely. Also, large events outside the circle can decrease the probability inside the circle if they are within a distance of approximately ξ. Note that the vertical axis is forecast probability in %.

Figure 7b. Timeseries illustrating the variation in time of forecast probabilities for $m \geq 7$ earthquakes within the selection circle for time interval of 1 year. Here the gradual increase in probability leading up to $m \geq 7$ events in the region, followed by sudden decrease following the event, can clearly be seen. This process is the analog of the stress accumulation and release process shown in Figure 3. The events causing the sudden decrease lie outside the selection circle in Figure 5, but they influence the probability over a defined correlation length of 400 km (Holliday et al., 2014). The m6.0 Napa earthquake caused the $m \geq 7$ probability to increase, since m6.0 is considered a "small" earthquake compared to an $m \geq 7$ earthquake. A general trend of declining probability can also be seen.

Query Location radio button. Clicking on this radio button produces two icons, a red "earthquake epicenter" icon, and a green "house" icon (Figures 8a,b). Moving these icons to positions of interest can be used to obtain a computation of ground motion from the earthquake at the red icon at the location of the green house icon. Location of the earthquake is given in latitude and longitude in the boxes below the words *Earthquake Source*. Magnitude, depth, and latitude-longitude of the earthquake can also be selected by entering the data directly into the text boxes. Options for hard or soft ground for the house location can be selected (this affects the ground shaking calculation). The result of the calculation can be seen in the box labeled *PGA* as a percentage of g, the surface acceleration of gravity.

Clicking on the *Shaking Intensity* bar/button produces a pop-up with data on the earthquake and house, the corresponding Modified Mercalli Intensity, and the source data.

Figure 8a. Query location button/bar. Clicking this button allows the user to place an earthquake (red icon) near a location (green house icon) and obtain an estimate of ground shaking. Output is Peak Ground Acceleration (PGA) in %g. For this screenshot, we have placed the earthquake icon at the epicenter of the 24 August 2014 Napa, Caliofornia, earthquake, and the house icon in the town of Napa. We set the magnitude of the earthquake at $m6.0$, and the depth equal to the epicentral depth of 10 km. We find PGA = 46.02%g, (red arrow) about equal to the observed value from strong motion records (Napa Shakemap, 2014).

Figure 8b. Clicking on the Shaking Intensity button/bar produces a report in a pop-up window summarizing the shaking intensity calculation.

Other Functions. Radio buttons can be found at the top left for displaying *Satellite Imagery* rather than the Google Map, *California Faults* from the UCERF2 database, and *Recent Earthquakes*. Note that UCERF3 fault map differs primarily from UCERF2 fault map by the addition of more small faults. Recent earthquakes markers are displayed as inverted tear drops. Color of the marker is keyed to magnitude, with hotter colors being larger magnitudes. Clicking on the marker gives information about the earthquake such as magnitude, time of occurrence and location in latitude-longitude.

Information on *Other Hazards* can also be displayed by clicking on the radio buttons in that section. The *GDACS* radio button displays icons provided by the United Nations Global Disaster Alert and Coordination System, together with the European Commission. Clicking on those icons gives small pop-ups with information about the various disaster incidents.

Wildfire - Current and Wildfire – 1 Week shows contours of fire hazard provided by the US Forest Service for current conditions and for conditions 1 week from the present. US FEMA flood zones can be displayed by clicking on that radio button. The flood zones become increasingly detailed as the zoom level is increased. Radon hazard can also be displayed as a contour map by clicking on that button.

GUIDE TO THE WEB APPS – HOME DAMAGE ESTIMATOR (www.openhazards.com/response)

The home damage estimator allows the user to examine the possible damage to their residence or other structure (Figure 9). There are basically two parts to this app. The first is the calculation of Peak Ground Acceleration and Spectral Acceleration via a Ground Motion Prediction Equation, which is carried out with a modified form of the attenuation relation published by Cua and Heaton (2009). The second part is based on the damage model by Graf and Lee (2009), and is modified to relate changes in building codes more closely to dates of construction.

Figure 9a. Home Damage Estimator. a) Placing the earthquake. b) Assigning structural details. c) Placing the earthquake and specifying the magnitude. d) Clicking on Create Report and viewing the pop-up summary.

There are 3 self-explanatory steps to follow in generating a report on possible damage:

1. **Locate House**. Move the (green) House icon to a location (Figure 9a). Either place the mouse cursor on the house and move it, or enter an address or a location and click *search*. The House icon will move to the specified location. In Figure 9a, we assume a location in Napa, California.
2. **Describe House**. Values for these fields are either filled in from Zillow, Inc. values (Zillow, 2014), or have default values (Figure 9b). If the values are incorrect, the user should fill in correct values. Note that the field "Structural Value" is the reconstruction cost of the structure, not the sale price. The user also needs to determine whether the House is located on relatively solid hard ground, or soft ground. Soft ground promotes more intense shaking. In Figure 9b, we assume the house was built in 1900 and had URM Bearing Wall framing, 2 floors, 1400 square feet, and was sitting on soft ground.

3. **Place Sample Earthquake**. For the last step, the user should move the red earthquake icon with their mouse cursor to a desired location near the house (Figure 9c). Note that both California faults and the global forecast are displayed for reference in deciding where to place the earthquake. The user can also select the magnitude of the earthquake from the menu at the bottom of the page. In Figure 9c, we place the earthquake icon at the south Napa epicenter and select the magnitude of $M = 6.0$
4. **Create Report**. Once the other steps have been completed, the user should click on the *Create Report* button and a pop-up page will appear with the results of the calculation (Figure 9d). This page can be printed using the printer icon in the upper right hand corner or saved to pdf. In Figure 9d, we see the pop-up summary page, showing that this house would be severely damaged by the shaking, suffering 55% damage to the value, a loss of $166,000 of the original $300,000 structural value.

The Home Damage Estimator can be used in various ways. A simple application of the tool will allow the user to determine what the loss is likely to be for a given set of earthquake scenarios.

Another use is to determine how much damage loss is likely to be avoided if seismic retrofitting is carried out. For example, if a residence were constructed in, say, 1950, the user would first enter that date on the "Describe House" screen. Then a report would be created for a specified earthquake configuration and the damage and loss noted. Next, the report would be re-created, but instead of using the date of 1950, the user would enter the current year 2014 instead. The calculation is then made assuming that the house conforms with the current building code, probably yielding a lower damage and loss estimate. The damage and loss from both calculations should then be compared and the differences used in deciding whether retrofitting is preferable to purchasing earthquake insurance.

GUIDE TO THE MOBILE APP – QUAKEWORKS
(Available on the Apple App Store)

The free Quakeworks mobile app can downloaded from the Apple App Store (Figure 10). An Android version will appear soon as well. The Quakeworks app has both a forecast and a home damage estimator tool. *Settings* at the top allows the users to choose distances in either miles or km.

Figure 10. QuakeWorks mobile app now available on the Apple App Store. The Android version will appear soon. The Forecast screen operates similarly to the Personal Earthquake Forecast web app. The Damage screen operates similarly to the Home Damage Estimator web app. Updates to the app may change the appearance in the future.

The **Forecast** screen is the equivalent of the Personal Earthquake Forecast web app, with the only difference being that it omits the calculation for $m \geq 8$. There is the usual geo-locate button (arrow), or the user can enter a location or address. Pressing the *Go* button activates the calculation and displays the result at the top of the screen.

Buttons can be seen to change the magnitude associated with the forecast to any of the choices:

- Magnitude ranges of $m \geq 6$, $m \geq 6.5$, or $m \geq 7$
- Future time intervals of 1 month, 1 year and 3 years into the future
- Distance ranges with radius of 50 km (miles), 100 km (miles) or 150 km (miles)

The **Damage** screen is equivalent to the Home Damage Estimator web app. The first screen is the *Map Viewer* and allows the user to enter the location of their residence or other structure, and to set the magnitude of the earthquake. The position of the earthquake is adjusted by placing a finger on the red earthquake icon and moving it on the map. The *arrow* or geolocate button will find the user's current location. The *House Info* screen draws information from Zillow and allows the user to update and correct information about their house or structure. If the user has used the arrow button, the House Info screen should contain information about the residence in which the user is located. Touching the *Report* button brings up the screen with home damage analysis.

Finally, a *FAQ* screen provides answers to questions about a number of different types of hazards and disasters, including earthquakes, tropical cyclones, wildfires, floods, and other events.

SUMMARY AND FUTURE PLANS

This paper has reviewed and discussed an operational, real-time earthquake forecast online at www.openhazards.com and its associated iOS7 mobile app, Quakeworks, available on the Apple App Store. We described the background to the method and basic model for the forecast. We then described the model for ground motion and building damage. Taken together, these models allow the development of operational forecast and damage analysis tools in a cloud-based setting. The web site represents a useful tool for rapid analysis of the seismic risk to persons and structures anywhere on earth. A second commercial site is in prototype stage at www.commercial.openhazards.com , including applications to the commercial real estate sector where structures are more complex, low- mid- and high-rise buildings must be considered, and soil liquefaction is a possibility.

Acknowledgements. The authors wish to thank the Open Hazards Group and its sponsors for support during the writing of this paper, and for the reduction to practice of the methods outlined here. The contributions of AD were supported by a NASA grant to JPL. The contributions of JBR were supported in part by a NASA grant to UC Davis. The authors would also like to thank the vast number of visitors to the site without whose interest this project would not have been brought to fruition.

References

ANSS, Earthquake Catalog Search - Accessed August 28, 2014, http://quake.geo.berkeley.edu/anss/catalog-search.html

Bevington, PR and Robinson, DK, 2003, *Data Reduction and Error Analysis in the Physical Sciences,* McGraw-Hill, Boston, MA.

Bufe, C.G. and Varnes, D.J. , 1993, Predictive modeling of the seismic cycle of the greater San Francisco Bay region, *J. Geophys. Res*., **98**, 9871-9883.

CMT , Earthquake Catalog Search - Accessed August 28, 2014, http://www.globalcmt.org/CMTsearch.html

Cua, G., and Heaton, T. ,2009, Characterizing average properties of southern California ground motion amplitudes and envelopes, Caltech EERL Report 2009-4.

Field, E.H. , Arrowsmith, R.J., Biasi, G.P., Bird, G.P., Dawson, T.E., Felzer, K.R., Jackson, D.D., Johnson, K.M., Jordan, T.H., Madden, C., Michael, A.J., Milner, K.R., Page, M.T., Parsons, T., Powers, P.M., Shaw, B.E., Thatcher, W.R., Weldon, R.J. and Zeng, Y. ,2014, Uniform California earthquake rupture forecast version 3 (UCERF3)-the time- independent model, *Bull. Seism. Soc. Am.,* **104**, 1122-1180.

Field, E.H., Overview of the Working Group for the Development of Regional Earthquake Likelihood Models (RELM) ,2007, *Seismol. Res. Lett., Jan/Feb*, **78,** 7-16.

Graf, W.P. and Lee, Y ,2009, Code-oriented damage assessment for buildings, *Earthquake Spectra*, **25**, 17-37.

HAZUS Software ,Accessed August 28, 2014, http://www.fema.gov/hazus

Holliday, J.R., K.Z. Nanjo, K.F. Tiampo, J.B. Rundle and D.L. Turcotte, ,2005, Earthquake forecasting and its verification, *Nonlin. Proc. Geophys.*, **12**, 965-977.

Holliday, J.R., Nanjo, K.Z. , Tiampo, K.F. , Rundle, J.B. and Turcotte, D.L. ,2005, Earthquake forecasting and its verification, *Nonlin. Proc. Geophys.*, **12**, 965-977.

Holliday, J.R., C.C. Chen, K.F. Tiampo, J.B. Rundle and D.L. Turcotte and A Donnellan, 2007, A RELM earthquake forecast based on Pattern Informatics, *Seism. Res. Lett*., **78**, 87-93.

Holliday, J.R., Graves, W.R. , Rundle J.B. and Turcotte, D.L. ,2014, Computing earthquake probabilities on global scales, *PAGEOPH*, accepted.

Hough, S. ,2010, *Predicting the Unpredictable: The Tumultuous Science of Earthquake Prediction*, Princeton University Press, ISBN 978-0-691-13816-9.

Joliffe, I. T. and Stephenson, D.B. ,2003, *Forecast Verification, A Practitioner's Guide in Atmospheric Science,* Wiley, ISBN 0-471-49759-2.

Lee, Y.T., Turcotte, D.L. , Holliday, J.R. , Sachs, M.K. , Rundle, J.B., Chen, C.C.and Tiampo, K.F. ,2011, Results of the Regional Earthquake Likelihood Models (RELM) test of earthquake forecasts in California, *Proc. Nat. Acad. Sci USA*, **108**, 16533-16538.

Napa Shakemap ,USGS: accessed 4 September, 2014, http://earthquake.usgs.gov/earthquakes/eventpage/nc72282711#shakemap

Rundle, J.B. ,1988a, A physical model for earthquakes: 1. Fluctuations and interactions, *J. Geophys. Res.*, 93, 6237 – 6254.

Rundle, J.B. ,1988b, A physical model for earthquakes: 2. Application to southern California, *J. Geophys. Res.*, 93, 6255 – 6274.

Rundle, J.B., Tiampo, K.F. and Klein, W. ,2007, Pattern Informatics and Cellular Seismology, A comparison of methods, *Trans. Am Geophys. Un. EOS*, **88**, 254.

Rundle, J.B., Holliday, J.R. , Graves, W.R. , Turcotte, D.L., Tiampo, K.F. and Klein, W. ,2012, Probabilities for large events in driven threshold systems, *Phys. Rev. E*, **86**, 021106

Scholz, C.H. ,1990, *The Mechanics of Earthquakes and Faulting*, Cambridge University Press, Cambridge, UK.

USGS Atom Feed ,Real Time Earthquake Feed-Accessed August 28, 2014, http://earthquake.usgs.gov/earthquakes/feed/v1.0/atom.php

WCRP ,World Climate Research Program, Accessed August 28, 2014, http://www.cawcr.gov.au/projects/verification/

WGCEP ,Working Group on California Earthquake Probabilities, accessed August 28, 2014, Reports can found at: http://www.wgcep.org/

Zechar, J.D. and Zhuang, J. ,2014, A parimutuel gambling perspective to compare probabilistic seismicity forecasts, *Geophys. J. Int.,* **199**, 60-68.

Zillow ,Zillow, Inc.: Accessed August 28, 2014, http://www.zillow.com

FIGURES AND CAPTIONS

Figure 1. Example of a Gutenberg-Richter (GR) cumulative magnitude-frequency for a large region and over a long time interval encompassing earthquakes up to magnitude M7.3. Recall that a cumulative magnitude-frequency relation represents the number of earthquakes having a magnitude greater than or equal to the magnitude indicated on the abscissa. Here the GR relation is for the large region of California, Nevada, southern Oregon and northern Baja Mexico, bounded by the latitudes 29^o and 42^o N, and the longitudes -127^o and -113^o W, over the time period from 1920 to August 7, 2014. The data are plotted as log N vs. M, where N is the number of earthquakes having magnitudes larger than M. The GR b-value for this Figure is: $b = 0.925 \pm 0.006$. At the large magnitude end, there are 2 earthquakes during this time that had magnitudes of M=7.3, the 28 June , 1992 Landers event, and the 21 July 1952 Kern County event.

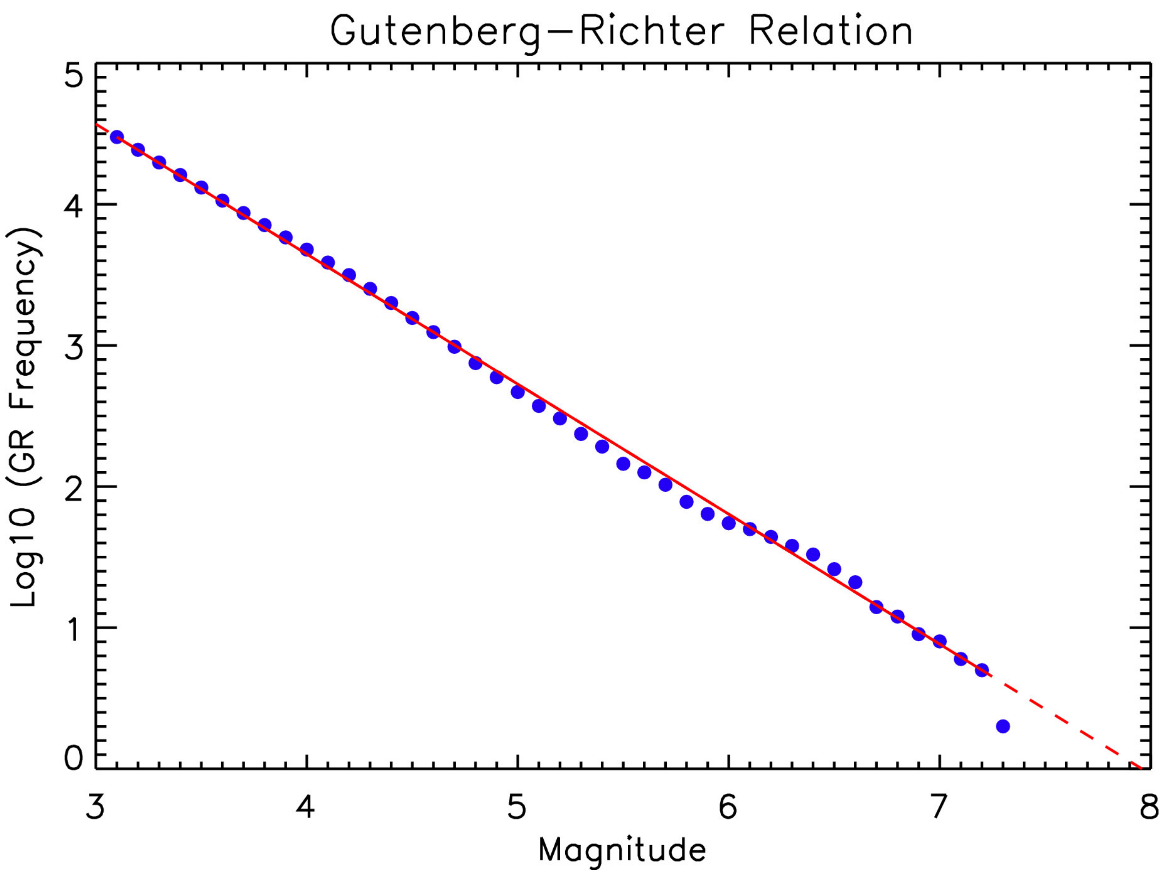

Figure 2. Example of a GR cumulative relation over a small region and a short time interval between two large earthquakes. This GR plot is for earthquakes within 200 km of the location centered on latitude 40.67^{o} N , longitude -125.01^{o} W, off the California coast. There were two recent earthquakes, an M6.5 on 10 January 2010, and a second M6.8 earthquake on 10 March 2014 within that 200 km radius circle. Figure 2 is very different from Figure 1, in that there is again a short scaling or linear region at the small magnitude end, but the intermediate and large magnitude events all fall well below the extrapolation of the scaling line. There is a very clear deficit of intermediate and larger magnitude earthquakes having magnitudes M>4.5 relative to the linear extrapolation implied by the small magnitude events. The GR b-value for line in this plot is:
$b = 0.531 \pm 0.013$

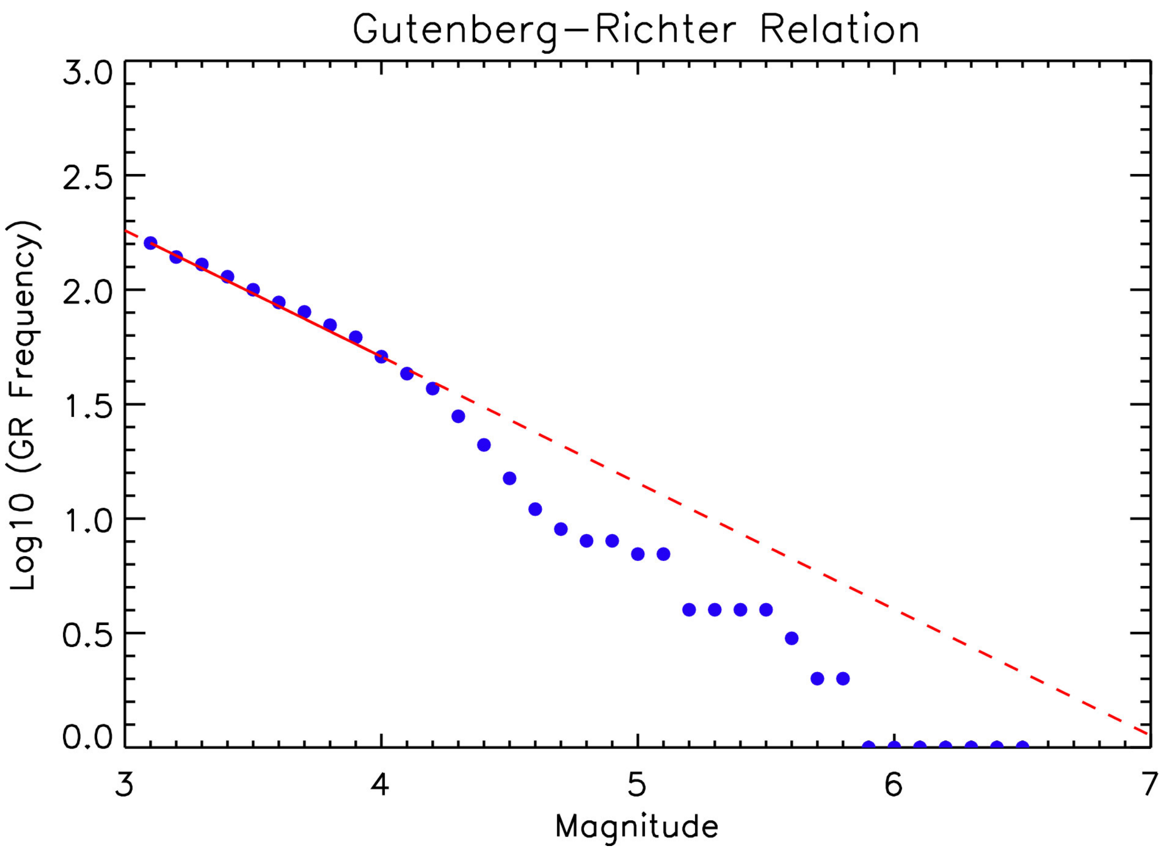

Figure 3. A classic representation of the time history of stress and slip on a simple isolated earthquake fault. Although the exactly repetitive nature of the stress and slip are now known to be an inaccurate, the basic ideas illustrated here are generally thought to represent the basic features of the earthquake cycle. The top plot shows the time history of stress accumulation and release, and the bottom plot shows the time history of cumulative slip on the fault. In the model, sudden slip occurs when the fault stress $\sigma = \sigma_F$, where σ_F represents the strength of the fault. During the earthquake, the slip suddenly increases (bottom figure), and the stress decreases to the residual value $\sigma = \sigma_o$. Two times are shown in the Figure 3, t_1, a time just prior to the earthquake, and t_2, a time just after the earthquake. *T* is the recurrence interval between earthquakes.

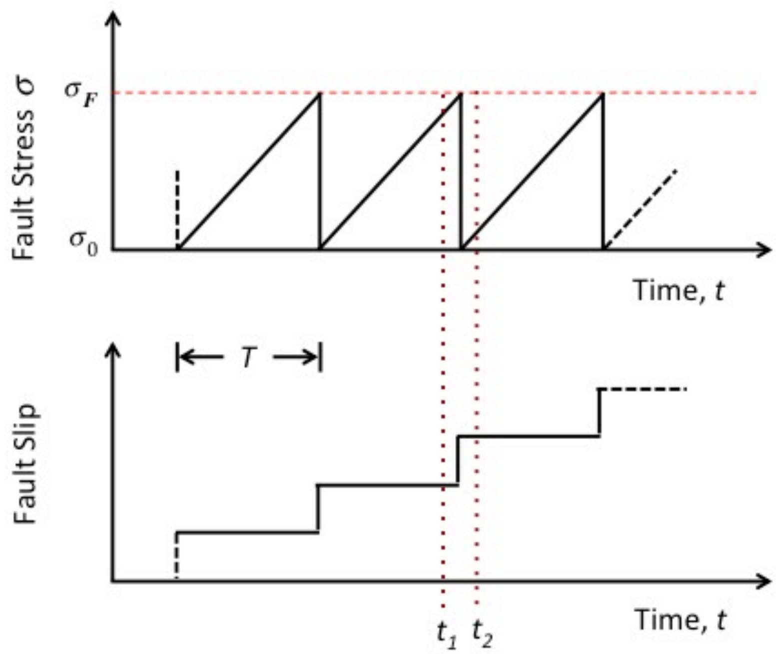

Figure 4. Personal Earthquake Forecast tool centered on the location of San Francisco, California. Small red star is the epicenter of the 24 August 2014 M6.0 south Napa earthquake. Low resolution global forecast contours are shown.

Personal Earthquake Forecast

San Francisco, ca

Go

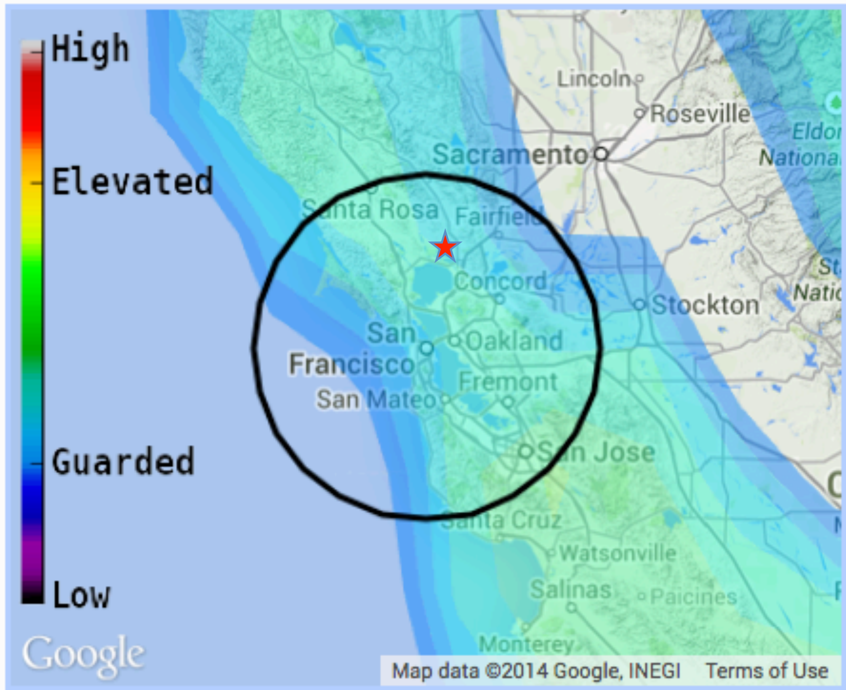

Probability of Earthquake Within 50 Miles of San Francisco, CA, USA

	1 Month	1 Year	3 Years
M≥5	0.41%	13.69%	74.39%
M≥6	<0.05%	1.25%	10.63%
M≥7	<0.05%	0.63%	5.41%
M≥8	<0.05%	0.06%	0.52%

Wed Sep 03 2014 14:12:41 GMT-0700 (PDT)

Figure 5. Hazard Viewer tool illustrating the use of a selection circle of radius 100 km around San Francisco, California, with additional display of forecast contours and UCERF2 fault system. The selection circle encompasses the epicenter of the 24 August m6.0 south Napa earthquake at upper right center of the circle (small red star). the calculations indicate that there is a 2.3% chance of a $m \geq 6$ earthquake within the selection circle within 1 year from September 3, 2014 (i.e., the period from September 3, 2014 to September 2, 2015). There is a 1.3% chance of an $m \geq 7$ earthquake during the same time period. Probabilities rise for the longer time interval of 3 years.

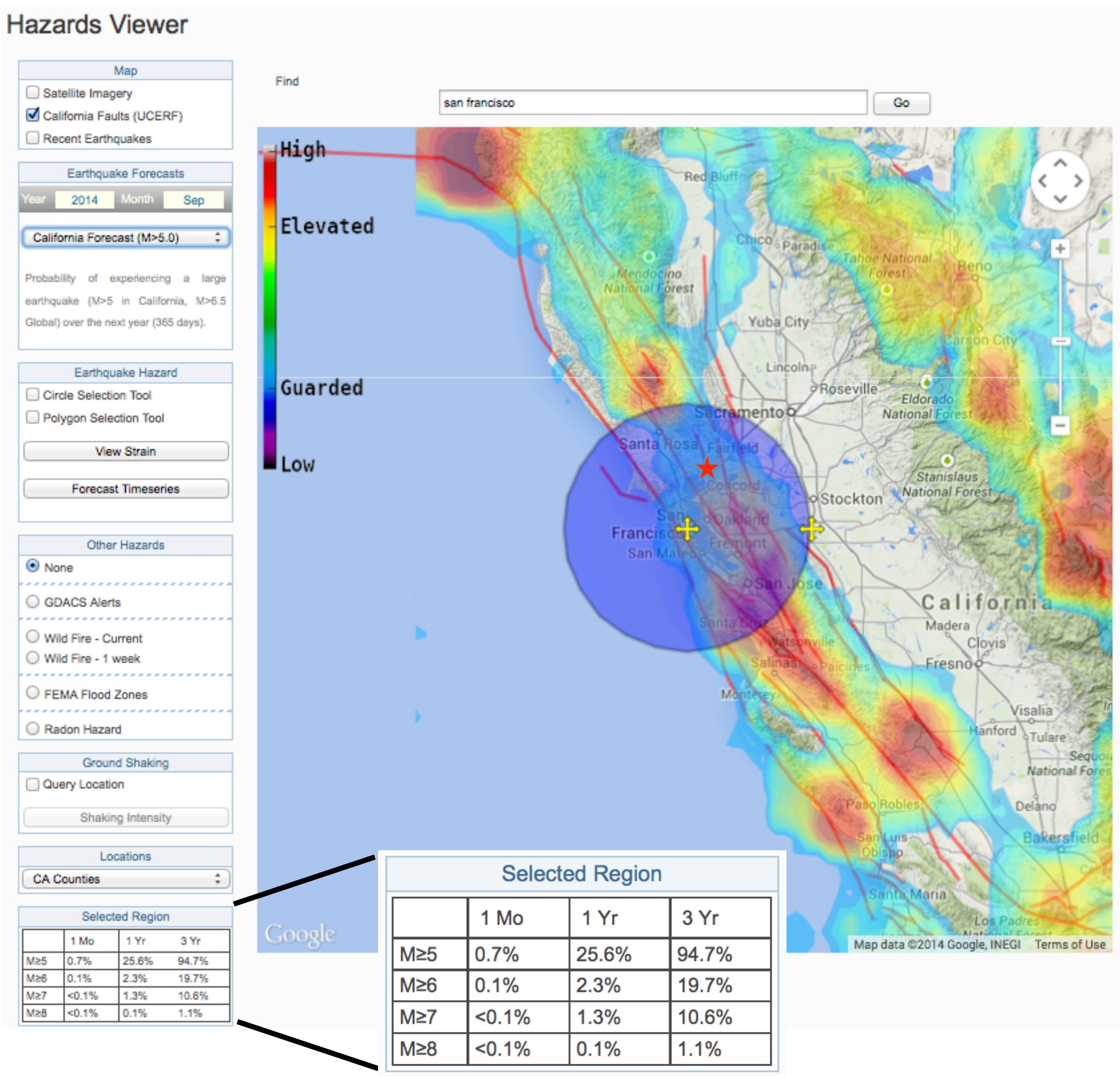

Selected Region

	1 Mo	1 Yr	3 Yr
M≥5	0.7%	25.6%	94.7%
M≥6	0.1%	2.3%	19.7%
M≥7	<0.1%	1.3%	10.6%
M≥8	<0.1%	0.1%	1.1%

Figure 6. Benioff strain release time series for events in the selection circle of Figure 5. The small yellow icon at lower right corner represents the 24 August 2014 M6 Napa, California earthquake. Magnitudes of earthquakes larger than 2 are also shown as a function of time from 2005 to present. The large step in strain release at the upper right hand side is due to the Napa earthquake.

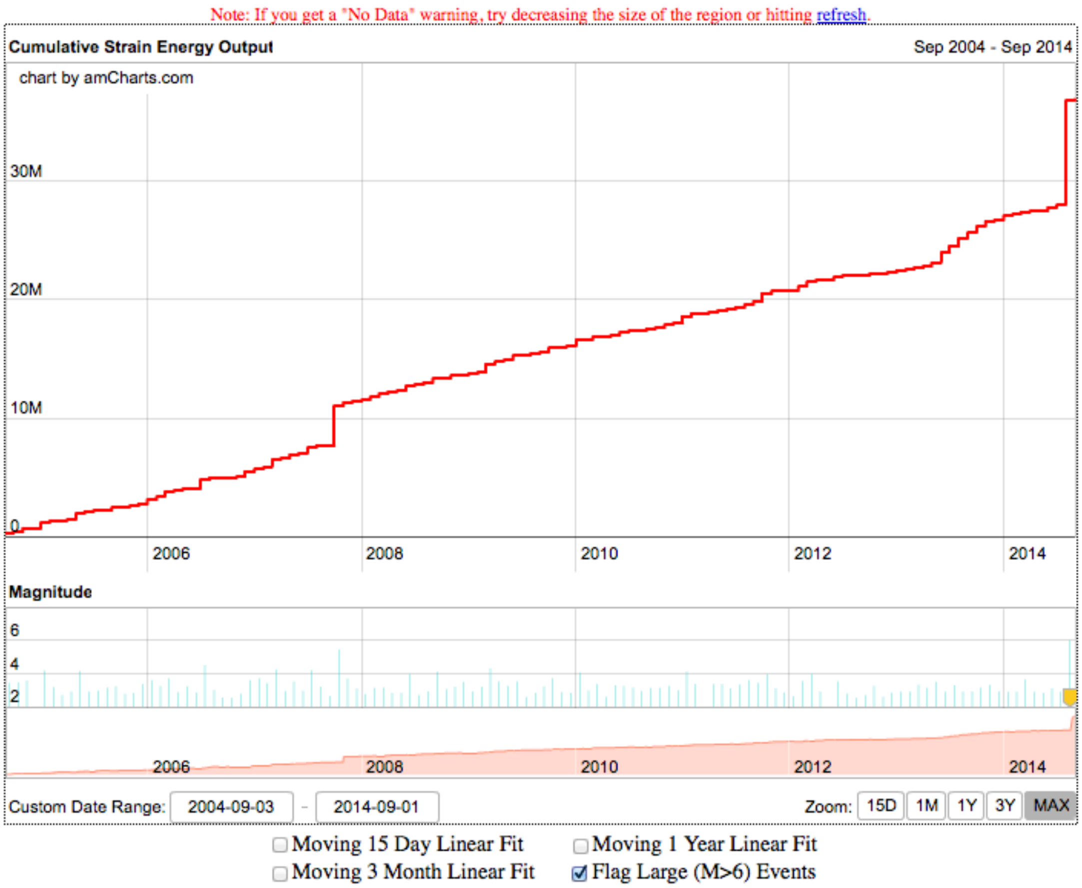

Figure 7a. Monthly timeseries illustrating the variation in time of forecast probabilities for $m \geq 6$ earthquakes within the selection circle for time interval of 1 year. The small yellow icon at lower right corner represents the 24 August 2014 m6.0 Napa, California earthquake. The M6 Napa earthquake caused the $m \geq 6$ probability to decrease, similar to Figure 3. A general trend of declining probability can also be seen, which is due to the occurrence of other large events in the region, outside the selection circle. These other large events influence the probability inside the selection circle by means of the correlation length ξ as described in Holliday et al. (2014). If events in the region become less frequent, the overall probability in the circle will tend to decrease over time, and conversely. Also, large events outside the circle can decrease the probability inside the circle if they are within a distance of approximately ξ. Note that the vertical axis is forecast probability in %.

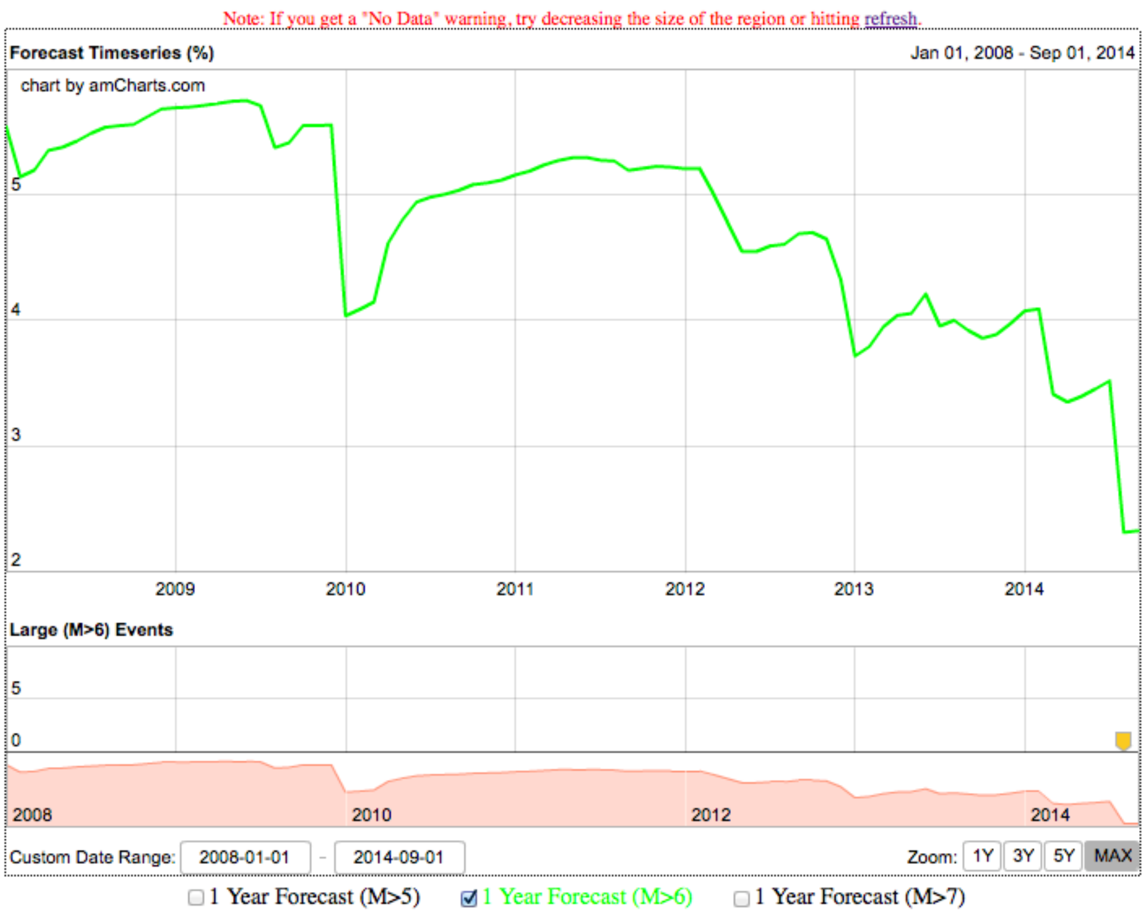

Figure 7b. Timeseries illustrating the variation in time of forecast probabilities for $m \geq 7$ earthquakes within the selection circle for time interval of 1 year. Here the gradual increase in probability leading up to $m \geq 7$ events in the region, followed by sudden decrease following the event, can clearly be seen. This process is the analog of the stress accumulation and release process shown in Figure 3. The events causing the sudden decrease lie outside the selection circle in Figure 5, but they influence the probability over a defined correlation length of 400 km (Holliday et al., 2014). The m6.0 Napa earthquake caused the $m \geq 7$ probability to increase, since m6.0 is considered a “small” earthquake compared to an $m \geq 7$ earthquake. A general trend of declining probability can also be seen.

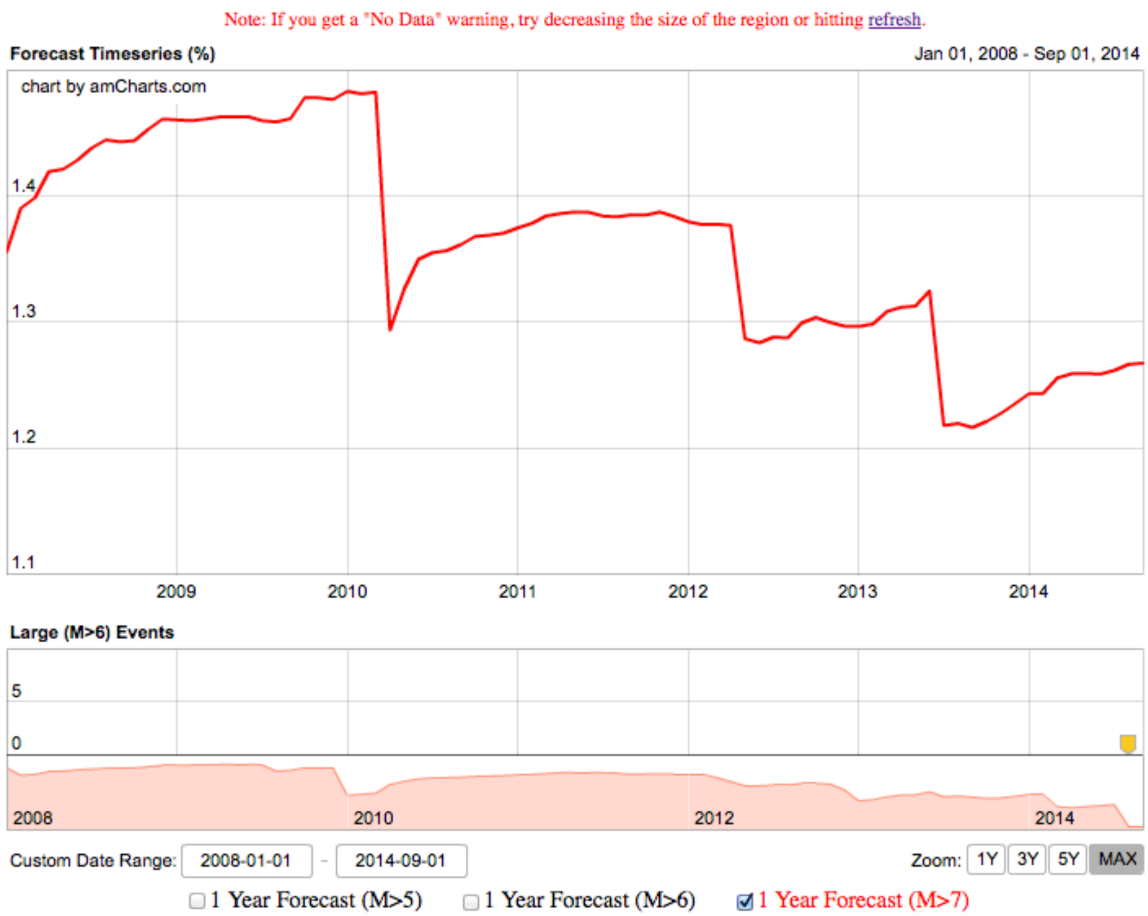

Figure 8a. Query location button/bar. Clicking this button allows the user to place an earthquake (red icon) near a location (green house icon) and obtain an estimate of ground shaking. Output is Peak Ground Acceleration (PGA) in %g. For this screenshot, we have placed the earthquake icon at the epicenter of the 24 August 2014 Napa, Caliofornia, earthquake, and the house icon in the town of Napa. We set the magnitude of the earthquake at $m6.0$, and the depth equal to the epicentral depth of 10 km. We find PGA = 46.02%g, (red arrow) about equal to the observed value from strong motion records (Napa Shakemap, 2014).

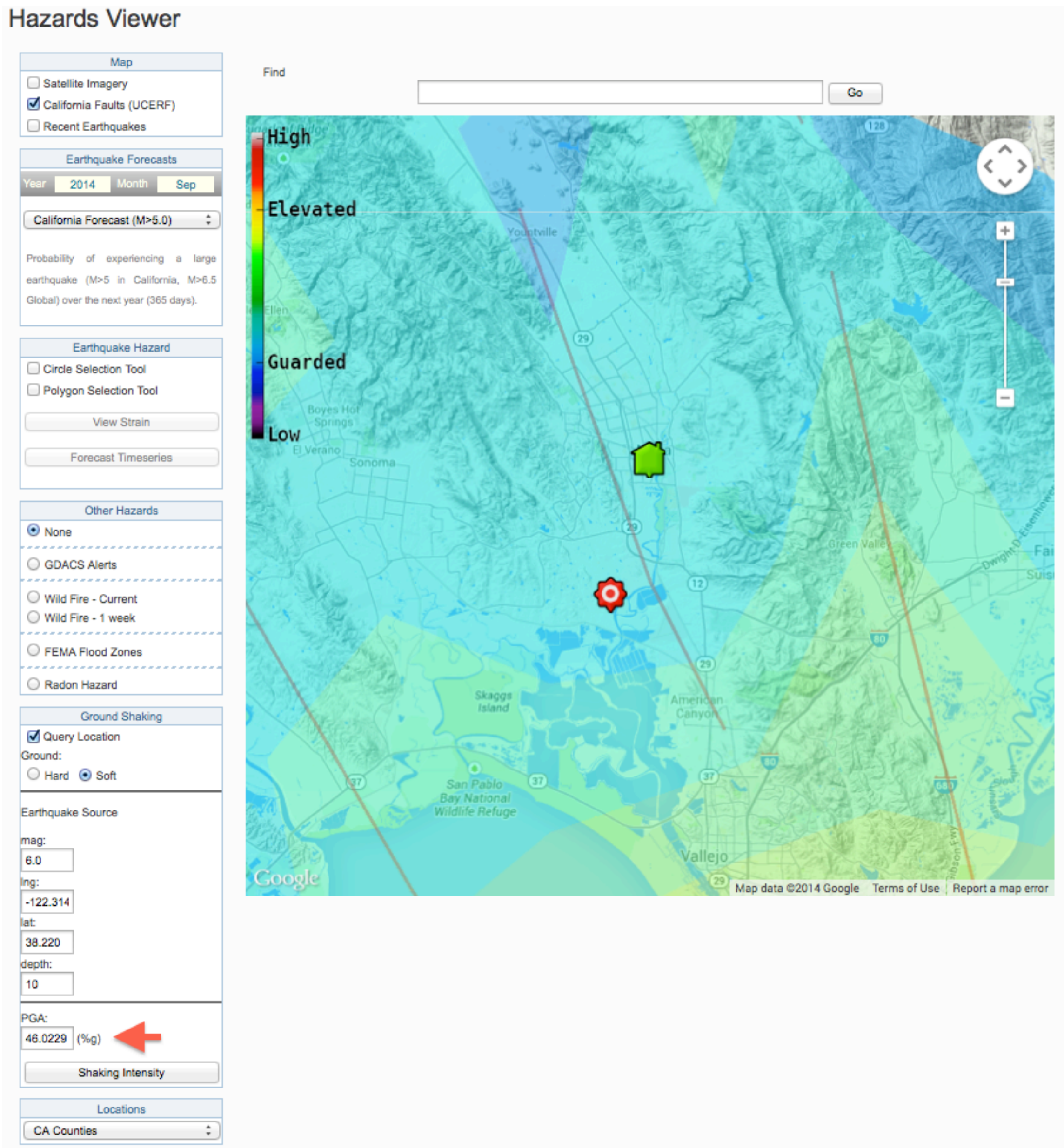

Figure 8b. Clicking on the Shaking Intensity button/bar produces a report in a pop-up window summarizing the shaking intensity calculation.

Risk Assessment For Likely Ground Shaking

Report Generated: Thu, 4 Sep 2014
Location: (38.284057477641426, -122.2906494140625)
Source: (38.21977630755083, -122.31388854980469)
PGA: 46.0229 (%g)
MMI: VIII

Steering of motor cars affected. Damage to masonry C; partial collapse. Some damage to masonry B; none to masonry A. Fall of stucco and some masonry walls. Twisting, fall of chimneys, factory stacks, monuments, towers, elevated tanks. Frame houses moved on foundations if not bolted down; loose panel walls thrown out. Decayed piling broken off. Branches broken from trees. Changes in flow or temperature of springs and wells. Cracks in wet ground and on steep slopes.

A descriptive table of Modified Mercalli Intensity is available from ABAG (Association of Bay Area Governments). A table of intensity descriptions with the corresponding peak ground acceleration (PGA) and peak ground velocity (PGV) used by the USGS is given below.

PERCEIVED SHAKING	Not felt	Weak	Light	Moderate	Strong	Very strong	Severe	Violent	Extreme
POTENTIAL DAMAGE	none	none	none	Very light	Light	Moderate	Moderate/Heavy	Heavy	Very Heavy
PEAK ACC.(%g)	<.17	.17-1.4	1.4-3.9	3.9-9.2	9.2-18	18-34	34-65	65-124	>124
PEAK VEL.(cm/s)	<0.1	0.1-1.1	1.1-3.4	3.4-8.1	8.1-16	16-31	31-60	60-116	>116
INSTRUMENTAL INTENSITY	I	II-III	IV	V	VI	VII	VIII	IX	X+

Figure 9a. Home Damage Estimator. a) Placing the earthquake. b) Assigning structural details. c) Placing the earthquake and specifying the magnitude. d) Clicking on Create Report and viewing the pop-up summary.

a)

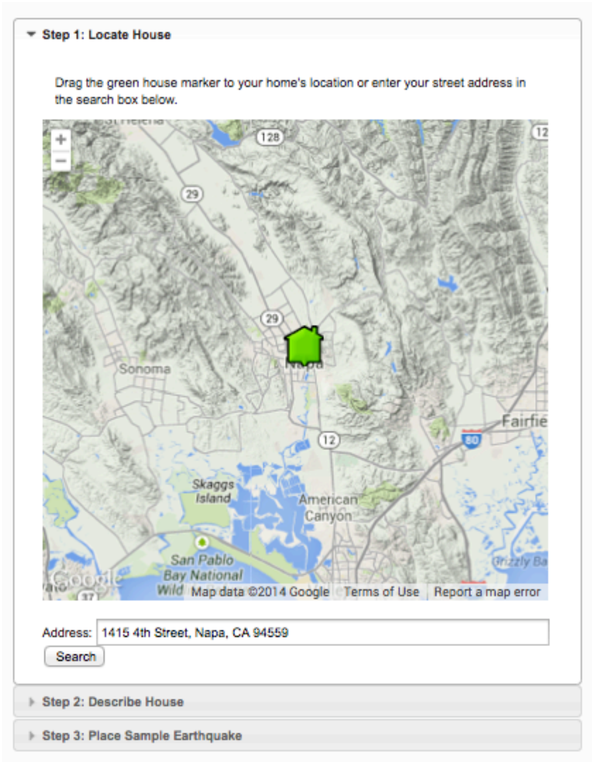

b)

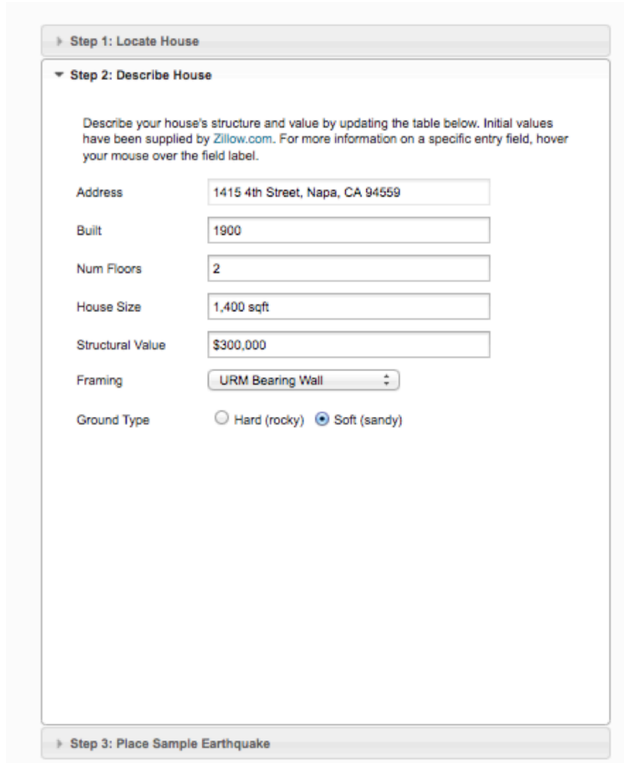

c)

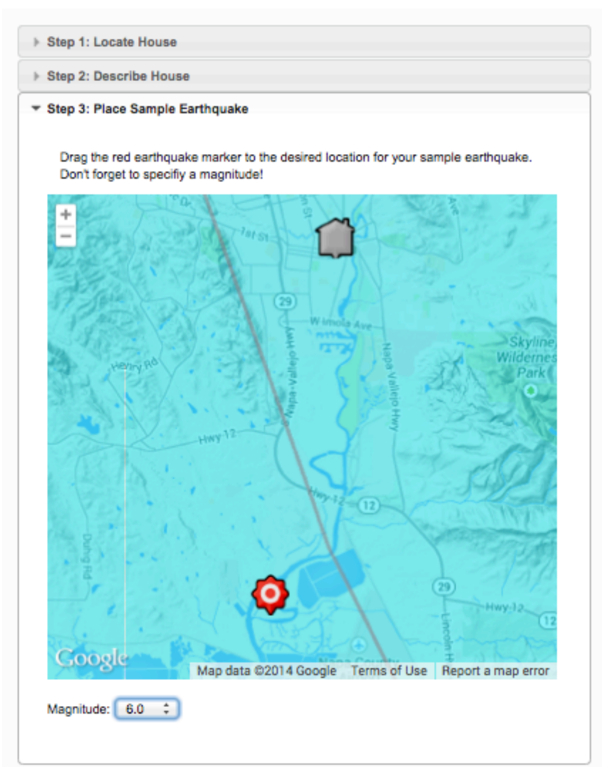

d)

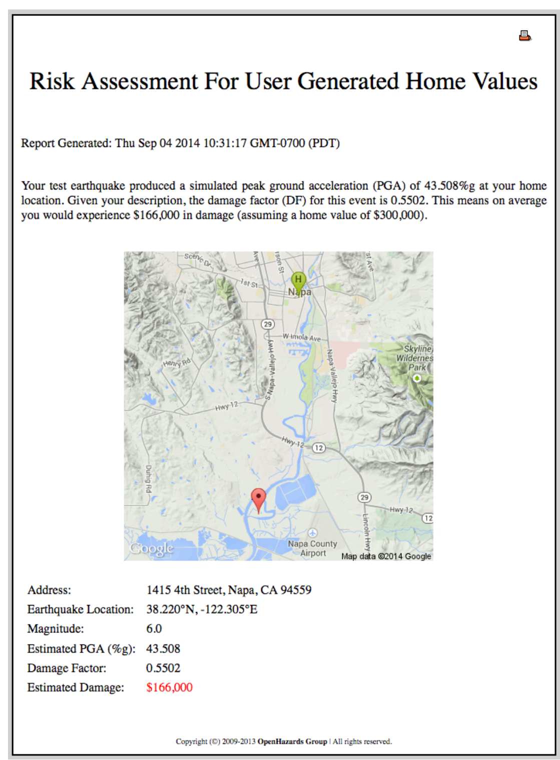

Risk Assessment For User Generated Home Values

Report Generated: Thu Sep 04 2014 10:31:17 GMT-0700 (PDT)

Your test earthquake produced a simulated peak ground acceleration (PGA) of 43.508%g at your home location. Given your description, the damage factor (DF) for this event is 0.5502. This means on average you would experience $166,000 in damage (assuming a home value of $300,000).

Address:	1415 4th Street, Napa, CA 94559
Earthquake Location:	38.220°N, -122.305°E
Magnitude:	6.0
Estimated PGA (%g):	43.508
Damage Factor:	0.5502
Estimated Damage:	$166,000

Figure 10. QuakeWorks mobile app now available on the Apple App Store. The Android version will appear soon. The Forecast screen operates similarly to the Personal Earthquake Forecast web app. The Damage screen operates similarly to the Home Damage Estimator web app. Updates to the app may change the appearance in the future.